

Characteristics of brush plated ZnTe thin films

K.R. MURALI, M. ZIAUDEEN*, N. JAYAPRAKASH
Central Electrochemical Research Institute, Karaikudi, 630 006, India

Published online: 17 February 2006

Zinc telluride thin films were deposited by the brush plating technique at a potential of -0.90 V (SCE) on conducting glass and titanium substrates at different temperatures in the range 30 – 90°C . The films were polycrystalline in nature with peaks corresponding to the cubic phase. Direct band gap of 2.30 eV was observed. XPS studies indicated the formation of ZnTe. Depth profiling studies indicated a uniform distribution of Zn and Te throughout the entire thickness. EDAX measurements were made on the films and it was found that there was a slight excess of Te. © 2006 Springer Science + Business Media, Inc.

1. Introduction

Zinc telluride is one of the II–VI group compound semiconductors that have been extensively studied for application in solar cell applications. It is a very good back contact for CdTe in heterojunction solar cells based on CdTe/CdS [1–3], since it has a small valence band discontinuity with CdTe and can be doped with copper to obtain low resistance [4–6]. Zinc telluride thin films have been deposited by several techniques like molecular beam epitaxy [7], electrode position [8–10], hot wall evaporation [11] and conventional vacuum evaporation [12], RF sputtering [13]. To our knowledge this is the first report on ZnTe films grown by brush plating technique. In this paper, structural, optical and morphological properties of brush plated ZnTe films are presented.

2. Experimental techniques

ZnTe films were deposited on conducting glass and titanium substrates using an aqueous solution of 0.5 M ZnSO_4 and 50 mM TeO_2 . The pH of the bath was adjusted to 2 by adding sulphuric acid. 10 ml of the precursor solution mixture was taken. The brush anode viz., graphite electrode wound with cotton was dipped in the solution and brushed over the cathode applying a potential of -0.90 V (SCE). Deposition potential was fixed on the basis of a previous report [9]. The deposition time was maintained as 15 min. The films were characterized by X-ray diffraction technique using a Phillips X-ray diffractometer and $\text{CuK}\alpha$ radiation, optical absorption studies were made using U 3400 Hitachi UV-Vis-NIR spectrophotometer, XPS studies were made using a VG ESCALAB MKII spectrometer with $\text{MgK}\alpha$ radiation, EDAX measurements were recorded with the

help of SEM attached with an EDAX microanalysis unit and AFM studies were made using Molecular Imaging system. The thickness of the films was in the range of 1.5 – 2.5 μm with increase of substrate temperature. Selective plating also known as brush plating, differs from traditional tank or bath plating in that the work piece is not immersed in a plating solution (electrolyte) instead, the electrolyte is brought into the part and applied by a hand-held anode or stylus, which incorporates an absorbent wrapping for applying the solution in the work piece (cathode). A direct current power pack drives the electrochemical reaction, depositing the desired metal on the surface of the substrate. In practice, movement between the anode and cathode is required for optimum results when plating, stripping, activating and so on. Currently a broad range of metals can be plated by brush plating. The key advantage of selective plating is portability. Many systems can be moved to various locations in a production facility or be transported to the job site. Selective plating is also versatile: it permits most electroplate types to be deposited onto any conductive substrate that can be touched with an electrode. Cast iron, copper, stainless steel and aluminum can be plated by this method and exhibit good adhesion. Limited adhesion can be obtained with other materials such as titanium, tungsten and tantalum.

Selective plating allows higher current densities than tank plating, which translates into higher deposition rates, unto 0.0100 mm/min. In addition, inherently precise thickness control permits plate buildup or repair without the need for subsequent machining. In regard to deposit hardness, 70 HRC trivalent chrome is available for selective plating of thick deposits.

* Author to whom all correspondence should be addressed.
0022-2461 © 2006 Springer Science + Business Media, Inc.
DOI: 10.1007/s10853-006-4434-5

Besides electroplating, selective plating systems can perform several other ancillary operations:

- Electro stripping for depleting of many metals and alloys.
- Anodizing for protecting aluminum alloys.
- Anodizing for protecting aluminum alloys.
- Electro milling for removing base metal, as in chemical milling.
- Electro etching for permanently identifying parts.
- Electro polishing for refining a surface chemically.

Depending on part size, dimensional considerations, and required surface characteristics all of these operations can be done with the same equipment and similar electrodes. Only the solutions are different. In many cases, an operator brush plate's only one part at a time. Nevertheless, selective plating is an effective and economical electroplating process when used in application for which it is assigned. These include plating parts that are too large to immerse in solution, plating a small area of a large component, and touching and repair of components, large or small that would cost too much to strip and manufacture. The largest parts ever plated are building domes. The process can also perform at higher production volumes.

Typical selective plating systems include a power pack, plating tools (called as styli or anodes), anode covers, specially formulated plating solutions, and any auxiliary equipment required for the particular application. To achieve optimum deposits, equipment should be designed expressly for selective plating. Power packs or rectifiers supply the direct current and are specially designed with the features and/or controls required by the process. Output voltage can be typically varied from 0–30 V, compared to direct tank plating power packs. Voltage control is extremely important because it regulates the current supplied

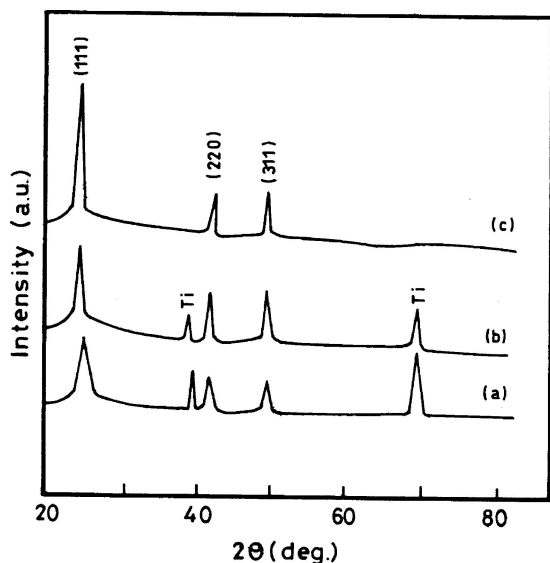


Figure 1 X-ray diffractogram of ZnTe films deposited at different temperatures (a) 30°C, (b) 50°C and (c) 90°C.

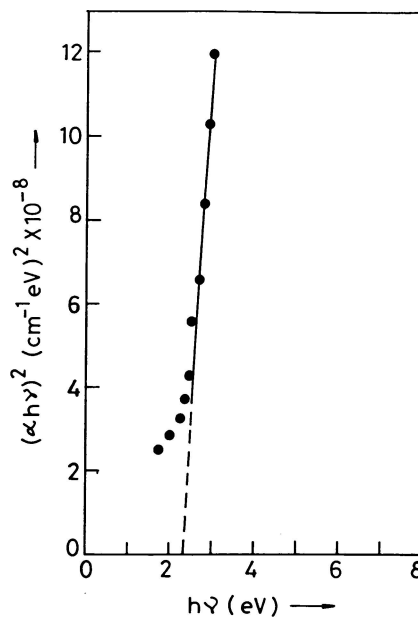


Figure 2 $(\alpha hv)^2$ vs $h\nu$ plot of ZnTe film deposited at a substrate temperature of 90°C.

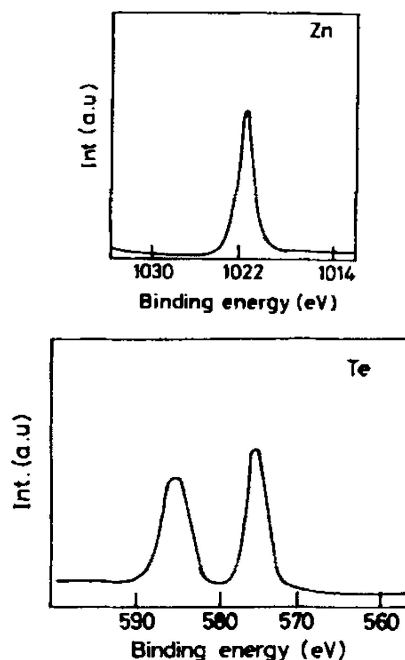


Figure 3 XPS spectrum of ZnTe films deposited at a substrate temperature of 90°C.

to the process. In turn, the amount of current consumed over time measured in ampere hour, determines the deposit thickness. A polarity reversing switch allows the operator to automatically change current flow direction, which is necessary in preparatory operations e.g., etching and demitting and in stripping.

The plating tool stylus must have an insulating handle and an anode material that is inert, insoluble in plating solutions, and able to carry high current. Graphite is by far the most practical choice for anode material. Graphite can be machined or shaped to fit the contour of the part

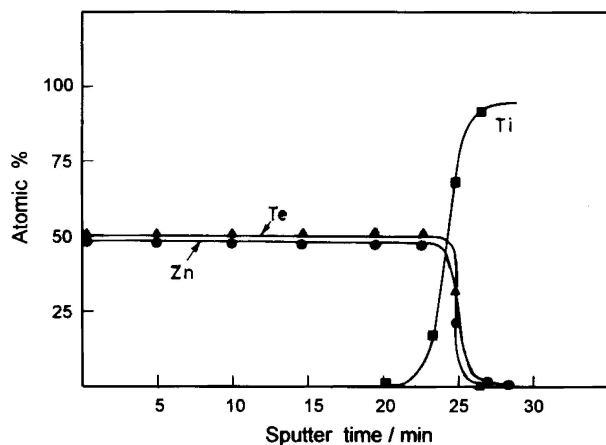


Figure 4 Depth profile of ZnTe film deposited at a substrate temperature of 90°C.

being processed. Stainless steel is much more durable, but it dissolves in certain plating solutions. The anode cover (wrapping materials) serve as an insulator between the anode and the cathode and help ensure smooth deposits at higher current densities. Because they hold the electrolyte, they must be absolutely free of oil and foreign materials. Various fibers like materials make suitable covers. Cotton works very well if it is sterile. Long fiber. Synthetic fibers such as polyester and nylon do not wet or hold electrolytes as well as cotton, but this does not preclude their use. Polyester felts is typically selected when the same anode will be used for numerous parts are to be plated. Most of these materials work well in the form of tube gaze as covers over cotton. Scotch brite has been used when heavy or hard deposits are required and it can also function as a burnishing tool, improving thru surface as plating continues. If a surface is soft and easily scratched, a different wrap should be chosen.

Controlling continuous movement between the anode and the work piece or cathode, is a key element in obtaining high quality brush plated deposits. However, quality also depends on plating within a specific current density range, so both varieties affect ultimate deposit quality. The visual appearance of the electrodeposits is also an indicator of quality. A dark grey or black deposit usually corresponds to a burnt deposit, which results from too high current densities or insufficient movement. In contrast inadequate current density or too much movement produces a generally shiny surface. Anode to cathode movement may be achieved manually or mechanically, such as by using turning equipment to provide a constant rotational speed for cylindrical parts. Another option is rotostylus which rotates the anode instead of the work piece.

For the plating process to be efficient the plating solution must flow between the anode and the area being plated. Solution can also be supplied by periodically dipping the plating tool into the electrolyte. However, the most efficient method is to pump the solution through the block anode and into the interface between the anode

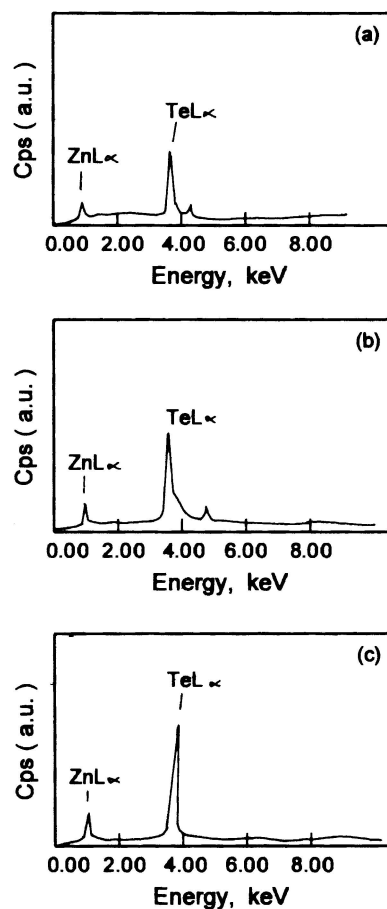


Figure 5 EDAX spectrum of ZnTe films deposited at different substrate temperatures (a) 30°C, (b) 50°C and (c) 90°C.

and the work piece. Plating of large areas at high current densities requires the use of a pump to re circulate the solution. This keeps the solution from overheating results in higher thickness buildup. In addition the process is faster. The thickness of a deposit can be controlled by monitoring the ampere hour meter. Each solution has a prescribed energy factor, which indicates how many ampere hours are required to deposit a given metal thickness on a given area.

3. Results and discussion

Structural studies were made using x-ray diffraction studies. Fig. 1 shows the XRD patterns of the films deposited at different substrate temperatures. Peaks corresponding to (111), (220) and (311) orientations of the cubic phase are observed. As the substrate temperature increases, the (111) orientation peak increases in intensity and the width of the peaks also decrease as the temperature of the substrate temperature increases. The crystallite size was calculated using Scherer's equation [14]. The crystallite size was found to increase from 40 nm –100 nm as the substrate temperature increases. The lattice constant was estimated to be 0.610 nm for the films deposited at a substrate

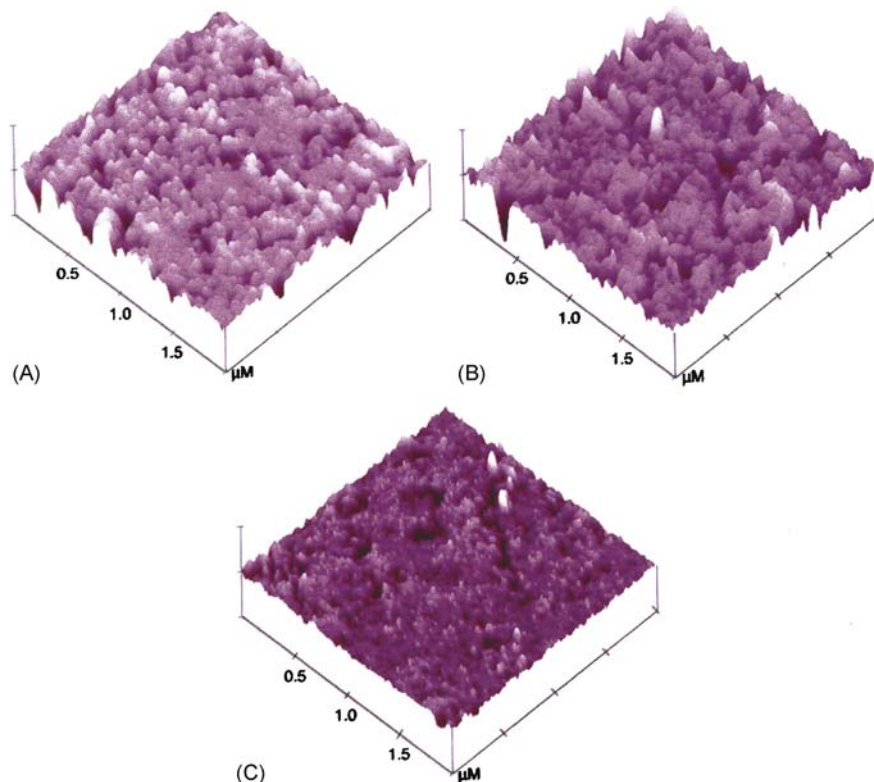


Figure 6 AFM image of ZnTe films deposited at different substrate temperatures (a)30°C, (b) 50°C and (c) 90°C.

temperature of 90°C. It is observed that the lattice constant is close to the value reported in the ASTM data [15].

Optical absorption spectrum of the films deposited on conducting glass substrates were recorded in the wavelength ranges 400–800 nm. Fig. 2 shows the $(\alpha h\nu)^2$ vs $h\nu$ plot for the films deposited at a substrate temperature of 90°C. The plot is linear indicating the direct band nature of the films. Extrapolation of the linear region to the energy axis indicated a band gap of 2.30 eV. This value is similar to the value obtained on single crystals [16].

X-ray photoelectron spectroscopic indicated the formation of ZnTe. Fig. 3 shows the XPS spectrum of ZnTe films deposited at 90°C. XPS studies indicated the Zn 3p and Te 3d peaks, which are in close agreement with the reported values for Zn and Te in ZnTe. Depth profiling was carried out at a sputter rate of 10 nm/min, this indicates a uniform distribution of Zn and Te throughout the thickness (Fig. 4). EDAX measurements yielded a composition of 49.5% Zn and 51.5% Te (Fig. 5).

AFM studies indicated that particle size increases as the substrate temperature increases (Fig. 6). Small crystallites of size 80 nm were observed for the films deposited at low temperatures. For the films deposited at 50°C, the crystallite size was 60 nm and for the films deposited at 90°C, the crystallite size increased to 120 nm, these results are slightly higher than the crystallite size determined from the XRD results. The surface roughness is high for the films deposited at low substrate temperatures compared to films deposited at high temperatures. More compact and uniform films are obtained at 90°C.

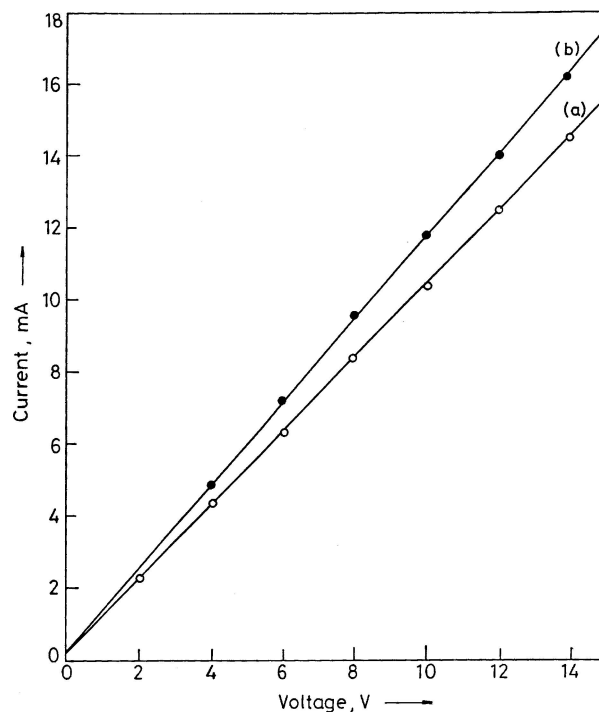


Figure 7 I-V characteristics of ZnTe films deposited at different substrate temperatures (a) 50°C and (b) 90°C.

The conduction mechanism in semiconductors can be understood by analyzing current- voltage plots. For single carrier injection at low voltages, the plot is generally a straight line showing the validity of Ohm's law. However,

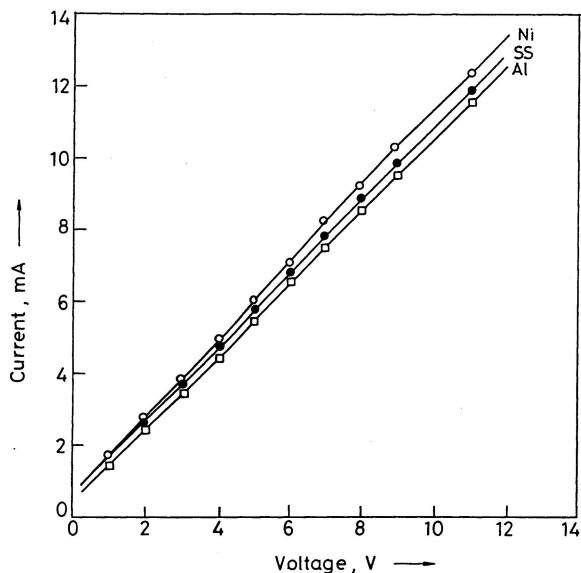


Figure 8 I-V characteristics of ZnTe films deposited on different substrates.

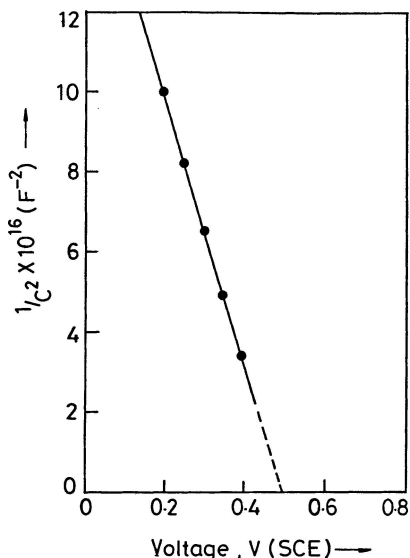


Figure 9 Mott-Schottky plot of ZnTe films deposited at a substrate temperature of 90°C.

at higher voltages some deviation is expected. The I-V characteristics of the films deposited at different substrate temperatures are shown in Fig. 7 The current measured for the applied voltages in the range 0–15 V was in the milliamperage range. At higher voltages the films get punctured and hence studies were restricted to only up to 15 V. Fig. 8 shows the I-V plots of ZnTe films deposited on different substrates like Al, SS and Ni. The linear behaviour is attributed to the filling of a discrete set of traps lying at or below the Fermi level. From the linear region, the bulk electrical conductivity is estimated to be in the range 4.0–6.0 mho cm⁻¹.

The semiconductor-electrolyte interfacial region is endowed with electrical heterogeneity on account of the existence of a depletion layer on the semiconductor side and a diffused double layer on the semiconductor side.

The overall capacitance of this region of photoelectric activity is made up of two distinct contributions from these space charge regions existing on either side of the interface. In view of the relatively much lower charge carrier density in the depletion layer, the experimentally measured capacitance of the semiconductor-electrolyte interfacial region is attributed to the semiconductor alone. The charge distribution in the depletion layer is altered when the semiconductor potential is varied. The semiconductor capacitance thus depends on the electrode potential; this dependence is usually expressed in terms of the Mott Schottky relationship

$$1/C^2 = 2/\epsilon\epsilon_0qN_D(V - V_{fb} - kT/q)$$

where N_D is the charge carrier density, q is the electronic charge, V_{fb} is the flat band potential, k is the Boltzmann constant, T is the absolute temperature, ϵ and ϵ_0 are the dielectric constants of the semiconductor and vacuum.

According to this relationship, $1/C^2$ vs V plot should be linear. The results obtained on ZnTe films are shown in Fig. 9 The slope of the Mott Schottky plot is negative which is characteristic of p-type semiconductors. Flat band potential was obtained by extrapolating the plot to voltage axis, Flat band potential was found to be 0.5V (SCE). The slope of the plot yielded a carrier density of 10^{15} cm⁻³.

4. Conclusion

The results of this investigation indicate that films of device quality can be deposited by the brush plating technique and the method can be scaled up for commercial exploitation. p-type films with high conductivity of the order of 4.0 mho cm⁻¹ can be obtained by this technique. Films with crystallite size in the range 50–150 nm can be easily deposited.

References

1. D. RIOUS, D. W. NILES and H. HOCHST, *J. Appl. Phys.* **73** (1993) 8381.
2. T. A. GESSERT and T. J. COUTS, in Proceedings of the 12th NREL Photovoltaic Program Review (1993) p. 345.
3. T. A. GESSERT, A. R. MASON, R. C. REEDY, R. MASTON, T. J. COUTS and P. SHEILDON, *J. Electron. Mater.* **34** (1995) 1443.
4. J. TANG, D. MAO, L. FENG, W. SONG, and J. U. TREFAY in Proceedings of the 25th PVSC, 13-17 May 1996, Washington DC (1996) p. 952.
5. L. FENG, D. MAO, J. TANG, R. T. CULINS and J. U. TREFAY, *J. Electron. Mater.* **25** (1996) 1442.
6. N. B. CHAURE, J. P. NAIR, R. JAYAKRISHNAN, V. GANESAN and R. K. PANDEY, *Thin Solid Films* **324** (1998) 78.
7. R. N. BICKNELL-TASSINS, T. A. KUHN and W. OSSAU, *Appl. Surf. Sci.* **36** (1989) 95.
8. B. M. BASOL and V. K. KAPUR, *Thin Solid Films*, **165** (1988) 237.

9. MICHAEL NEUMANN SPALLART and C. KONIGSTEIN, *ibid.*, **265** (1995) 33.
10. T. MAHALINGAM, V. S. JOHN, S. RAJENDRAN, G. RAVI and P.J. SEBASTIAN, *Surface Coatings Technol.* **155** (2002) 245.
11. P. LINK, T. SCHMIDT, S. BANER, H. P. WAGNER, H. LEIDERER and W. GEBHARDT, *J. Appl. Phys.* **72** (1992) 3730.
12. U. PAL, S. SAHA, A. K. CHAUDHARI, V. V. RAO and H.D. BANERJEE, *J. Phys. D* **22** (1989) 965.
13. H. BELLAKHDER, A. OUTZOURHIT and E.L. AMEZAIN, *Thin Solid Films* **382** (2001) 30.
14. A. GUINER, *Theorie et Technique de la Radiocristallographie*, Editions Dunod, Paris (1969).
15. ASTM X-ray powder data 15-746, 19-1482, 4-554.
16. K. SATO and S. ADACHI, *J. Appl. Phys.* **73** (1993) 926.

*Received 30 April
and accepted 20 June 2005*